Deterministic and stochastic dynamics of linear polarizations emitted by single-mode VCSELs subject to orthogonal optical injection

P. Pérez[1,2], A. Quirce[1,2], A. Valle [1*], and L. Pesquera[1].
[1]Instituto de Física de Cantabria, CSIC-Universidad de Cantabria, Avda. Los Castros s/n, E-39005, Santander, Spain.
[2] Departamento de Física Moderna, Universidad de Cantabria, Avda. Los Castros s/n, E-39005, Santander, Spain

ABSTRACT

We present a theoretical and experimental study of the polarization-resolved nonlinear dynamics of a 1550nm single-mode linearly polarized VCSEL when subject to orthogonal optical injection. Anticorrelated (correlated) dynamics between the two linear polarizations emitted by the VCSEL is found for negative (positive) frequency detuning. Our theoretical analysis show that deterministic dynamics with appreciable values of the standard deviation of the period of the signal can be found for negative values of the frequency detuning. We study the effect of spontaneous emission noise on the dynamics by analyzing the dependence of the average and standard deviation of the interpulse time on the injected power. We find that in general the effect of spontaneous emission noise is to increase the standard deviation of the interpulse time.

Keywords: Semiconductor lasers, vertical-cavity surface-emitting laser (VCSEL), polarization switching, injection locking, nonlinear dynamics, interpulse time, correlation.

INTRODUCTION

Semiconductor lasers have been studied in the last years due to their various applications in optical communications and also because they can exhibit a rich variety of non linear behaviors [1]. These behaviors are usually induced by modulation of the bias current, optical and opto-electronic feedback or the injection of light from an external source. One of the most interesting types of semiconductor lasers are the vertical-cavity surface-emitting lasers (VCSELs). A lot of interest has been paid because of their nonlinear dynamics and their special characteristics, like single-mode longitudinal operation, circular beam profile, ease of fabrication of 2D-arrays, low fabrication cost, etc. [2]. Also, when VCSELs are compared to edge-emitting semiconductor lasers, they show additional degrees of freedom, for example, the presence of multiple transverse modes and the direction of the polarization of the emitted light. Very interesting phenomena related to transverse modes and polarization can appear in these devices. The direction of the light's polarization is able to change when the bias current is changed [3-4]. Also, mode-locking between transverse modes [5] and the appearance of turn-off-induced pulsations when the bias current is modulated [6-7] have been reported.

In this work we have considered external optical injection. If light emitted by another laser is injected to a VCSEL, its operational characteristics can be improved. External optical injection can be used to reduce the laser linewidth or the mode partition noise, for example, or for enhancing the modulation bandwidth [8-11]. It is important to remark that with this technique these improvements are reached without modifying the laser design. On the other hand, external optical injection is also interesting from the fundamental point of view, because it can lead the emergence of a wealth of complex nonlinear dynamics. These are period doubling, quasiperiodicity, chaos, polarization switching (PS), stable injection locking (SL) and optical bistability [12-34]. Early experiments and numerical simulations were done for a polarization of the injected light is parallel to that of the VCSEL [12-13] (this is called "parallel injection"). However, recent experiments considering the called "orthogonal injection" technique have been performed. In this configuration,

*e-mail: valle@ifca.unican.es; phone 34 942 201465; fax: 34 942 200935

the linearly polarized external light is injected orthogonally to the linear polarization of a free-running VCSEL [14]. The orthogonal optical injection on long-wavelength VCSELs has received so much interest because of his applications in optical telecommunication networks [26-34]. In these studies the devices had large values of the birefringence parameter and they emitted in a single linear polarization over the whole bias current without optical injection.

In these systems stability maps are used to analyze the non linear dynamics. In the maps the different behaviors are represented as a function of the power of the injected light and the detuning between the frequency of the injected signal and the free-running frequency of the orthogonal mode of the VCSEL. The maps have been built using the RF spectra of the total power emitted by the laser to find the boundaries of the different dynamical regimes [31-35], like periodic dynamics, PS and irregular (possibly chaotic) behavior. Simultaneous temporal traces, RF and optical spectra [35] of the total power and both polarizations have been measured in order to analyze the dynamics in more detail. In this work we pay special attention to the temporal traces of the power. We extend the study of the correlation properties between polarizations and, specially, the study of the average of interpulse time and its standard deviation. On another hand, we perform a theoretical analysis (numerical simulations) in order to study the effect of spontaneous emission noise on the dynamics, by analyzing the dependence of the average and standard deviation of the interpulse time on the injected power.

Our paper is organized as follows. A summary of the experimental results reported in [32,34,35] for the nonlinear dynamics for small and large values of the bias current are analyzed in section II. In section III we present a theoretical analysis using numerical simulations. Finally, in section IV, a summary and conclusions are presented.

II. SUMMARY OF EXPERIMENTAL RESULTS [32,34,35]

We have used all-fibre set-up in order to inject light from a tunable laser into a quantum-well 1550 nm VCSEL. All the set-ups used in [32,34,35] are similar (see fig 1). The same commercially available VCSEL (Raycan) has been used in all our experiments. A laser driver and a temperature controller control the VCSEL bias current and temperature, respectively. The temperature is held constant at 298 $^{\circ}$K during the experiments. With these set-ups we can inject light from a tuneable laser into a VCSEL with orthogonal polarization. Later, the light emitted by the VCSEL can be splitted into the two polarizations (parallel and orthogonal) and both polarizations and the total power can be directed to an oscilloscope with bandwidth of 6 GHz (two similar photodetectors were connected before it for measuring simultaneously time traces), to a RF spectrum analyzer or to a high-resolution optical spectrum analyzer (BOSA).

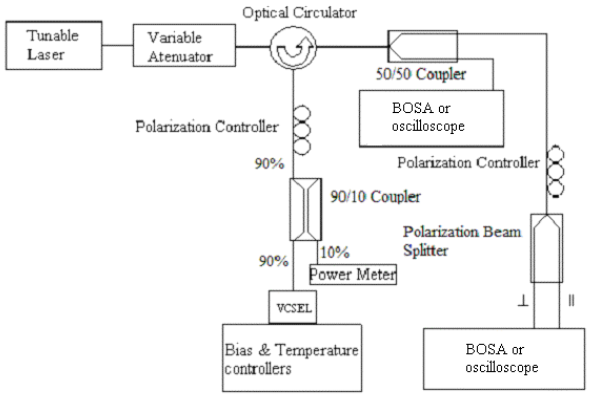

Fig. 1. Experimental set-up of orthogonal optical injection in a VCSEL.

The L-I curve of the free-running VCSEL is shown in [32, Fig. 2a]. The VCSEL is a single-transverse mode laser, with threshold bias current of I_{th}=1.64 mA. The laser emits in a linear polarization along the whole current range (called "parallel" polarization). Fig. 2(b) of [32] shows the optical spectrum of the VCSEL biased at 8 mA. The spectrum shows the peak of the lasing mode (with parallel polarization) at wavelength $\lambda_{\parallel}$ = 1536.6 nm. The other small peak corresponds to the mode with "orthogonal" polarization and its wavelength ($\lambda_{\perp}$) is shifted 0.49 nm with respect to the parallel one. This value is very large in comparison to those reported in short-wavelength devices [23].

The dynamical behavior of our system is reported in the stability maps [32,34-35] for different values of the bias current applied to the VCSEL. RF spectra of the total power are used to separate different dynamical regimes. The optical injection is characterized by its strength, (the value of the optical power arriving at the VCSEL, P_{inj}) and by its frequency, ν_{inj}. We define the frequency detuning as $\Delta\nu = \nu_{inj} - \nu_{\perp}$, where $\nu_{\perp}$ is the frequency of the perpendicular polarization. In these stability maps different dynamical behaviors are plotted in the $\Delta\nu$ - P_{inj} plane. The stability map of Fig. 2 of [34] shows that periodic (period 1 and period doubling) behaviour, irregular and possibly chaotic dynamics, and stable locking regions (SL) appear in this system.

In this section we summarize the experimental results of [32,34-35]. We have extracted some results of the power time traces measurements for illustrating the topics of interest in this work. We have studied the averaged interpulse time (<T>), its standard deviation (σ_T), and the correlation properties between times traces of the power of both polarizations (orthogonal $P_{\perp}(t)$ and parallel $P_{\parallel}(t)$). The interpulse time is defined like the time between two consecutive peaks of the temporal trace with a maximum above certain threshold value, previously chosen (This threshold value is selected in order to avoid the measure of this time between peaks caused by fluctuations). The correlation properties have been analyzed in terms of the cross correlation function:

$$C(\tau) = \frac{\overline{\left(P_{\parallel}(t+\tau) - \overline{P}_{\parallel}\right)\left(P_{\perp}(t) - \overline{P}_{\perp}\right)}}{\sigma_{\parallel}\sigma_{\perp}} \tag{1}$$

where the bar means time averaging operation and $\sigma_i^2 = \overline{\left(P_i(t) - \overline{P}_i\right)^2}$, i=||, ⊥. In this work we are interested in the value of (1) for the case of zero delay.

The figure 2 shows the summarized experimental results. Each column represents fixed values of bias current and frequency detuning. In each column, the upper plot has a lower P_{inj} value than the lower one. In fig. 2(a) and (d) we have the results for bias current of 8 mA and frequency detuning 5 GHz, with P_{inj} 96.1 μW and 127.6 μW, respectively. These plots show correlated periodic dynamics in both linear polarizations. As it can be seen, the average of the interpulse time has been reduced with the increase of P_{inj} (from 0.19 ns to 0.187 ns), and the standard deviation of T has values close to 7 ps. In table 1 the values of <T>, σ_T and C(0) are shown for these cases and some other studied in [34]. For this bias current and positive detuning, a positive correlation is found, and a reduction of <T> as P_{inj} increases (i. e., the period of the periodic signal decreases). This can be explained in terms of the "frequency pushing" effect [34].

Figs. 2(b) and (e) show the time traces for a negative value of the frequency detuning, $\Delta\nu$= -2 GHz, and for bias current I=4 mA, with P_{inj} 35.5 μW and 53.6 μW, respectively. In fig. 2(b) can be seen a non-sinusoidal periodic dynamics for both polarizations, in contrast to the positive $\Delta\nu$ case. Unlike in the case of positive detuning, now when P_{inj} is increased, both <T> and σ_T grow. The increase of <T> can be explained in terms of a "frequency pulling" effect [34]. Also, another important difference is that time traces of the power of the polarizations are anticorrelated. In table 1 the values of <T>, σ_T and C(0) are shown for these cases and some other studied in [34]. In fig. 2(e) the system is in an irregular regime, as we can see in the RF spectra in [34].

Finally, in figs. 2(c) and (f) the cases for $\Delta\nu$= -1.5 GHz, I=8 mA and P_{inj} 67.6 μW and 84.0 μW are shown, respectively. In fig. 2(c) a P2 regime is shown, and in fig. 2(f) we have a clear irregular and possibly chaotic dynamic. Similarly to the previous case, both <T> and σ_T grow as P_{inj} is increased, and a strong anticorrelation is found between polarizations (see table 1).

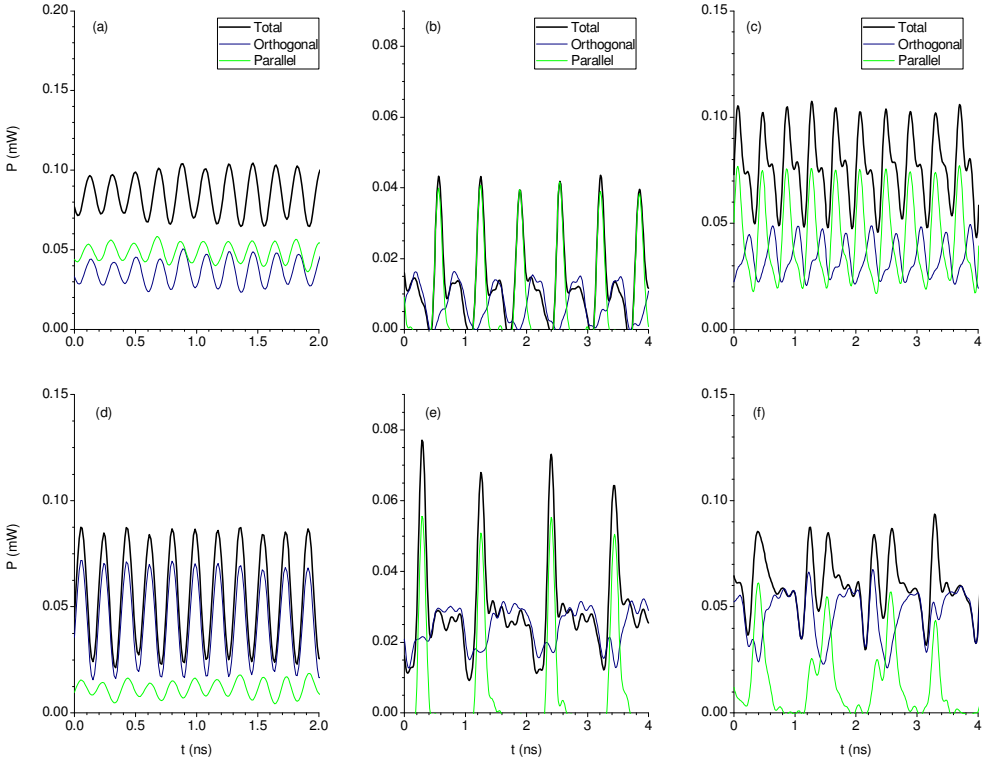

Fig. 2. Experimental time traces of the total power and of the power of both linear polarizations. Several values of injected power, frequency detuning and bias current are considered: (left column) I=8 mA, $\Delta\nu$ = 5 GHz (a) P_{inj}= 96.1 μW (d) P_{inj}= 127.6 μW, (center column) I=4mA, $\Delta\nu$ = -2 GHz (b) P_{inj}= 35.5μW (e) P_{inj}= 53.6 μW, (right column) I=8mA, $\Delta\nu$ = -1.5 GHz (c) P_{inj}= 67.6 μW (f) P_{inj}= 84.0 μW.

I/mA	Δν/GHz	P_{inj}/μW	<T>/ns	σ_T/ps	C(0)
4	-2	26.9	0.52	17	-0.54
		35.5	0.66	12	-0.51
		42.4	0.93	40	-0.48
		53.6	1.04	96	-0.50
8	-1.5	58.5	0.326	7	-0.37
		67.6	0.404	10	-0.47
		84.0	0.38	200	-0.67
	5	96.1	0.19	7	0.75
		127.6	0.187	6	0.65
		197.3	0.168	6	0.24

Table 1: Averaged interpulse time (<T>), standard deviation (σ_T), and correlation coefficient (C(0)) for different experimental cases.

As a conclusion of this section, we can remark two fundamental aspects. When $\Delta\nu$ <0 anticorrelated behavior between the power of both linear polarizations is clear. However, when $\Delta\nu$ >0 correlation between both linear polarizations is found. On the other hand, when $\Delta\nu$ <0, <T> increases with P_{inj}. The opposite behavior is found when $\Delta\nu$ >0. The correlation characteristic behavior can be explained in terms of competence between polarizations [34].

III. THEORETICAL RESULTS

In this section we are going to analyze from a theoretical point of view the average of interpulse time and its standard deviation obtained from the temporal trace of the total power and the correlation properties corresponding to the two linearly polarized modes emitted by the VCSEL subject to orthogonal optical injection. By using simulations we can study these quantities with and without spontaneous emission noise. Our rate equation model for the polarization of a VCSEL is based on the spin-flip model (SFM) [36]. Parameters of the model can be chosen such that the free-running VCSEL emits in the *y*-polarization, so orthogonal optical injection is obtained by considering an external field polarized along the *x* direction. The SFM model equations with orthogonal optical injection are given by

$$\frac{dE_x}{dt} = -(\kappa + \gamma_a)E_x - i(\kappa\alpha + \gamma_p)E_x + \kappa(1 + i\alpha)(NE_x + inE_y) + \kappa E_{inj}e^{i\Delta\omega t} + F_x \tag{2}$$

$$\frac{dE_y}{dt} = -(\kappa - \gamma_a)E_y - i(\kappa\alpha - \gamma_p)E_y + \kappa(1 + i\alpha)(NE_y - inE_x) + F_y \tag{3}$$

$$\frac{dN}{dt} = -\gamma\left[N(1 + |E_x|^2 + |E_y|^2) - \mu + in(E_yE_x^* - E_xE_y^*)\right] \tag{4}$$

$$\frac{dn}{dt} = -\gamma_s n - \gamma\left[n(|E_x|^2 + |E_y|^2) + iN(E_yE_x^* - E_xE_y^*)\right] \tag{5}$$

Where the noisy terms are:

$$F_x(t) = \frac{1}{\sqrt{2}}(F_+ + F_-) = \sqrt{\frac{\beta_{sp}\gamma}{2}}\left(\sqrt{(N+n)}\xi_+(t) + \sqrt{(N-n)}\xi_-(t)\right) \tag{6}$$

$$F_y(t) = \frac{-i}{\sqrt{2}}(F_+ - F_-) = i\sqrt{\frac{\beta_{sp}\gamma}{2}}\left(\sqrt{(N-n)}\xi_-(t) - \sqrt{(N+n)}\xi_+(t)\right) \tag{7}$$

$E_{x,y}$ are the two linearly polarized slowly varying components of the field and N and n are two carrier variables. N accounts for the total population inversion between conduction and valence bands, while n is the difference between the population inversions for the spin-up and spin-down radiation channels. The internal VCSEL parameters are as follows: κ (=125 GHz) is the field decay rate, γ_e (=0.67 GHz) is the decay rate of N, γ_s (=1000 GHz) is the spin-flip relaxation rate, α (=2.2) is the linewidth enhancement factor, μ is the normalized injection current, γ_a (=2 GHz) is the linear dichroism and γ_p (=192 GHz) is the linear birefringence. Fluctuations due to spontaneous emission (with a fraction of spontaneous emission photons that are coupled into the laser mode of $\beta_{sp} = 10^{-4}$) are included in our calculations by $\xi_+(t)$ and $\xi_-(t)$ (complex Gaussian noise terms of zero mean and time correlation given by $\langle\xi_i(t)\xi^*_j(t')\rangle = 2\delta_{ij}\delta(t-t')$). The optical injection parameters are E_{inj} and $\Delta\omega$. E_{inj} is the injected field amplitude and $\Delta\omega$ is defined as the difference between the angular frequency of the injected light, ω_{inj}, and a reference angular frequency intermediate between those of the *x* and *y* linear polarizations, i.e. $\Delta\omega = \omega_{inj} - (\omega_x + \omega_y)/2$. We have integrated Eqs. (2)-(5) by using the same numerical method for stochastic differential equations used in Ref. [34] with an integration time step of 0.01 ps.

We have chosen parameters based on those reported by R. Al-Seyab et al. [33] for a long-wavelength VCSEL similar to our device. With our parameters the free-running VCSEL is emitting in the parallel polarized mode (*y* mode) for all the bias current values, as in the experimental situation. Also, the frequency of the parallel polarized mode is higher than that of the orthogonal linear polarization (*x* mode): $\nu_y > \nu_x$, like for the VCSEL used in our experiments. Unlike in experiments, in simulations we can study the dynamics with noise ($\beta_{sp} = 10^{-4}$) and without noise ($\beta_{sp} = 10^{-40}$), in order to analyze the effect of the spontaneous emission noise in the behavior of the laser.

First of all, we did simulations of similar cases to experimental ones in order to study the behaviors of <T>, σ_T and C(0), for comparing with the experimental cases. In the figure 3 are plotted the results of our simulations with and without noise of the three magnitudes remarked. We have considered three cases: in the first column are the results for a frequency detuning of -2 GHz and a normalized bias current of 2.44 (that corresponds to the experimental case of fig. 2(a)-(d)); in the second column the values of frequency detuning and bias normalized current are -2 GHz and 4.88,

respectively (that corresponds to the experimental case of fig. 2(b)-(e)) and in the third column we have a frequency detuning of -2.7 GHz and bias normalized current of 2.44 (this case does not have an exact correspondence to an experimental one, but we have included it because of its interesting dynamics).

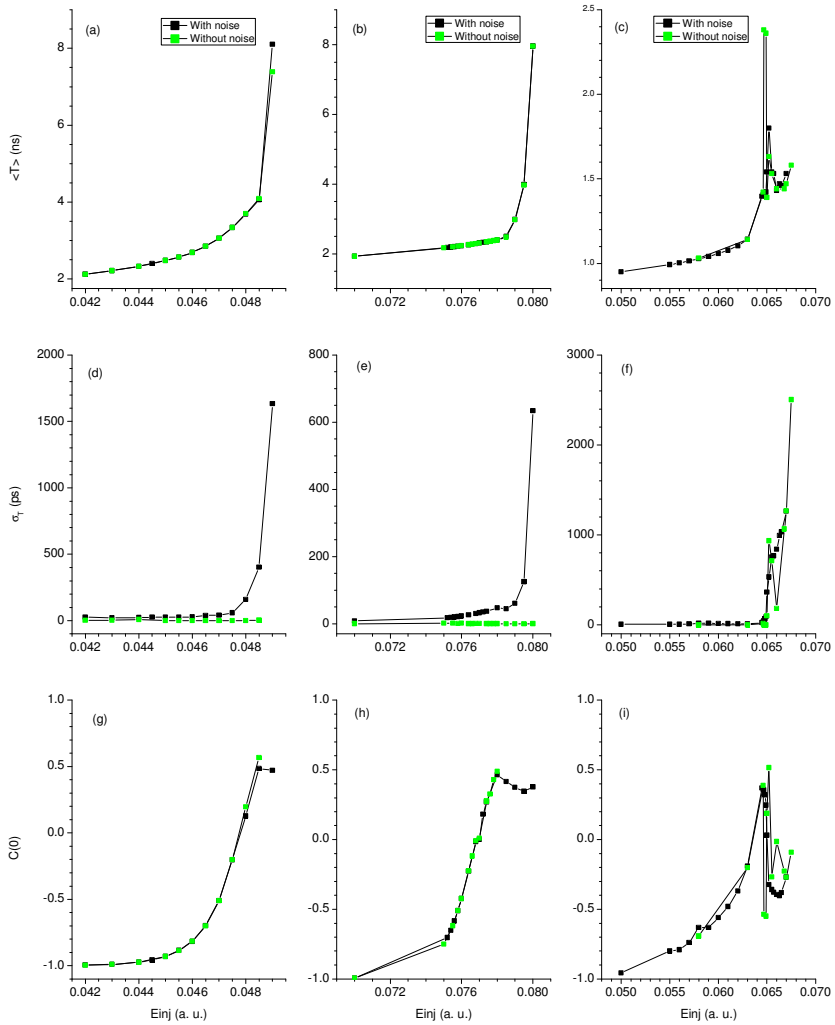

Fig. 3. Averaged interpulse time (<T>), standard deviation (σ_T), and correlation coefficient (C(0)) for simulation cases. Several values of frequency detuning and bias normalized current are considered: (left column) μ=2.44, $\Delta\nu$= -2 GHz, (center column) μ =4.88, $\Delta\nu$= -2 GHz, (right column) μ =2.44, $\Delta\nu$= -2.7 GHz.

As we can see in fig. 3(a)-(d)-(g), with a normalized bias current of 2.44 and frequency detuning of -2 GHz, the tendencies found for the case with noise are like those reported in the experimental cases of bias current 4 mA and frequency detuning -2 GHz (see table 1). The mean value and dispersion of the interpulse time grow with the strength of the injection. A negative correlation is obtained for a range of values of P_{inj}. However, positive values of C(0) are obtained when the injected power increases. In the case without noise, the same behavior has been obtained, with the exception of the interpulse time deviation. This magnitude does not increase with the strength of injection without noise: its value remains between one and four picoseconds. So, in this case, it is clear that the effect of spontaneous emission noise is to increase the interpulse time deviation, i. e., increase the dispersion of the time between consecutive pulses.

An analogue behavior is found for the case of normalized bias current 4.88 and frequency detuning -2 GHz (fig. 3(b)-(e)-(h)), which corresponds approximately to the experimental case with bias current 8 mA and frequency detuning -1.5

GHz (see table 1). A negative correlation is also obtained for a range of values of P_{inj}. However, the behavior of C(0) with the injected power is the opposite to the experimental case. Like the previous results, the only difference between the cases with and without noise is the behavior of the interpulse time deviation. While in the case with noise it grows sharply when the strength of injection is increased (it reaches the value of 600 ps), in the study without noise it stays around 0.5 ps, which is a very low value. So again, the principal effect of spontaneous emission noise is to increase the interpulse time deviation.

We now study the case with a normalized bias current of 2.44 and a frequency detuning of -2.7 GHz (fig. 3(c)-(f)-(i)). This frequency detuning has not been analyzed in the experimental case. As it can be seen, now the behavior is different (more complex) that the previously analyzed cases. For small values of E_{inj} the behaviors are similar to the previous cases, but for values in above 0.064 strange behaviors appear. For example, in some points the value of the interpulse time deviation without noise is larger than the one with noise. So now the effect of spontaneous emission noise is not only to increase σ_T but to change substantially the dynamics, as we will show below. In order to understand these behaviors, we have analyzed time traces of the total power and both polarizations and their RF spectra. In fig. 4 are shown the results without noise for -2.7 GHz frequency detuning and 2.44 normalized bias current and values of E_{inj} larger than 0.064. For values smaller than 0.064, the behaviors are periodic orbits and period doubling, like in the experimental cases previously analyzed.

The first case in fig. 4(a)-(b) is a regime that has not been seen in the experimental measurements: a period three. The strength of injection is 0.065. The appearance of period 3 is clear in the RF spectrum (fig. 4(b)), where a strong peak is observed at 0.73 GHz and two weaker peaks at 0.49 and 0.24 GHz (also some harmonics are observed). This period three obviously affects the interpulse time deviation, which reaches the value of 101.45 ps. We present a histogram of the interpulse time (fig. 5) in order to show that three groups of values of T appear. It is important to remark that in this case the value of interpulse time deviation is not a good indicator of the "irregularity" of the power temporal trace. It is easy to observe that the large value of σ_T is due to the existence of the sequence of three peaks which is repeated along the trace (which are separated three different times, as shown in histogram of fig. 5). So, because of these conclusions, the real period (the time every three pulses) and its standard deviation have been calculated, obtaining values of 4.18 ns and 46.41 ps, respectively. It is important to note that the value of the standard deviation of the period is less than the one for σ_T, but it cannot be neglected.

When the strength of the injection is increased (fig. 4(c)-(d)), the system presents an irregular behavior. No periodicity is observed in the temporal traces of total power and polarizations. This results in a large interpulse time deviation (712.6 ps). Also, very broad RF spectra are obtained (fig. 4(d)).

If E_{inj} is increased, a periodic dynamic is obtained again (fig. 4(e)-(f)). In the temporal traces of total power and polarizations (fig. 4(e)) single pulses can be seen, with a possible period 4, because in the RF spectra (fig. 4(f)) appear peaks at 0.70 GHz, 0.35 GHz (half frequency) and an incipient peak at 0.17 GHz (half frequency of 0.35 GHz). For larger values of frequency some harmonics are obtained. Similar to the case of fig. 4, a period of 5.78 ns has been calculated (which corresponds to the inverse of the frequency of 0.17 GHz in the RF spectrum) with standard deviation of 0.16 ps.

Finally, with a strength of injection of 0.0668 (fig. 4(g)-(h)) the periodic regime is broken and an irregular and possibly chaotic dynamics is obtained. In this case, temporal traces (fig. 4(g)) show irregular packets of pulses combined with plane zones. This irregular behavior is also reflected in the RF spectra (fig. 4(h)), which are very broad and with very weak peaks. The system presents this type of behavior until the strength of injection 0.068, where PS and SL are simultaneously reached.

After the analysis of the dynamic without noise, similar simulations, now with noise, have been done in order to understand the effect of spontaneous emission in the behavior of the system. In figure 6 the results for similar cases to fig. 4 are plotted but in the presence of noise. Fig. 6(a)-(b) illustrates a case close to the one of fig. 4(a)-(b). Solitary and double pulses appear in the temporal trace of the total power (fig. 4(a)). This "intermittency" results in the broad RF spectra (fig. 6(b)) and a great value of the interpulse time deviation (533 ps).

Increasing the strength of injection a similar case to fig. 4(c)-(d) is reached (fig. 6(c)-(d)). The situation is very similar to

the previous case (fig. 6(a)-(b)), with broad RF spectra (fig. 6(d)) and solitary pulses mixed with couple of pulses in the temporal traces of powers (fig. 6(c)).

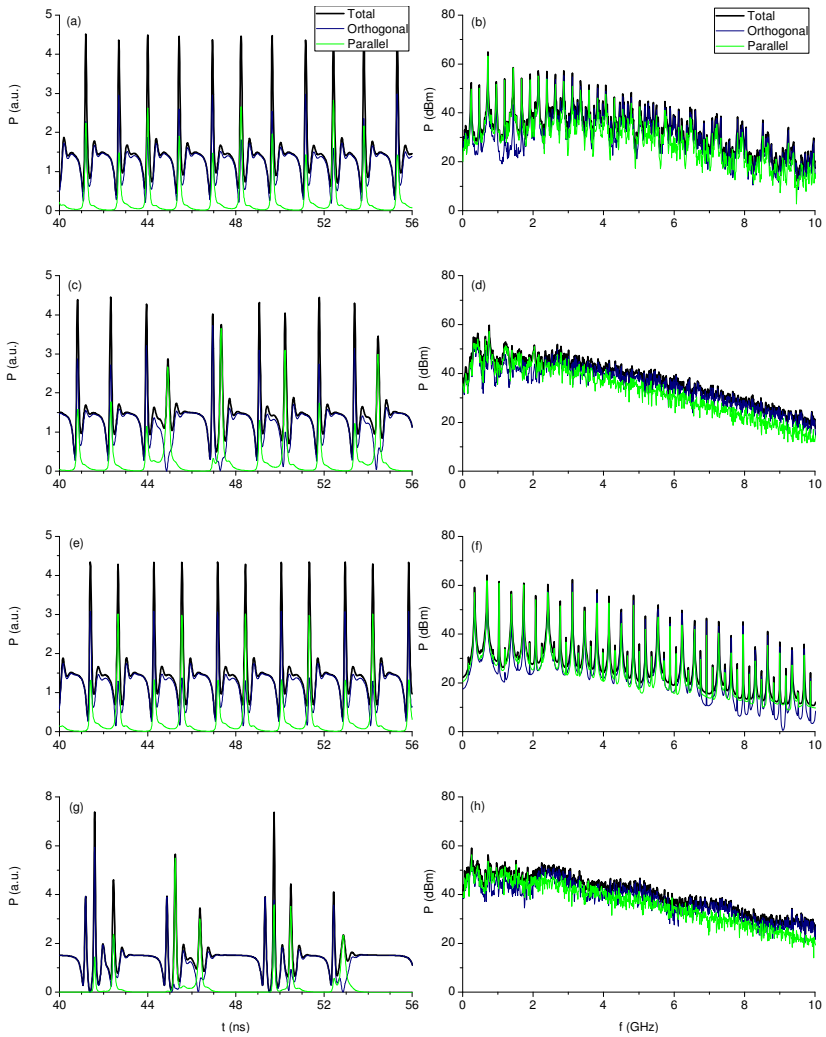

Figure 4: (left column): Temporal traces (right column): RF spectra. Total and both polarizations powers are shown. Values of E_{inj} are: (a,b) 0.065, (c,d) 0.0655, (e,f) 0.066, (g,h) 0.0668. Simulation with μ=2.44 and Δν=-2.7 GHz, without noise.

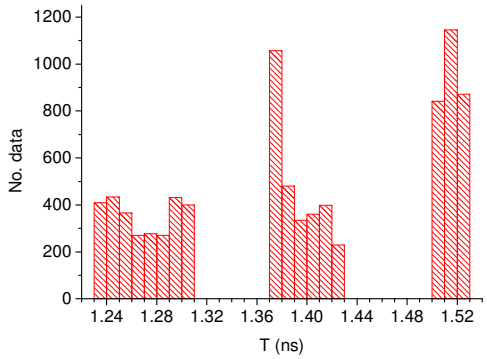

Figure 5: Histogram of the interpulse time for the case of fig. 4(a), i.e. μ=2.44, Δν=-2.7 GHz and E_{inj}=0.065.

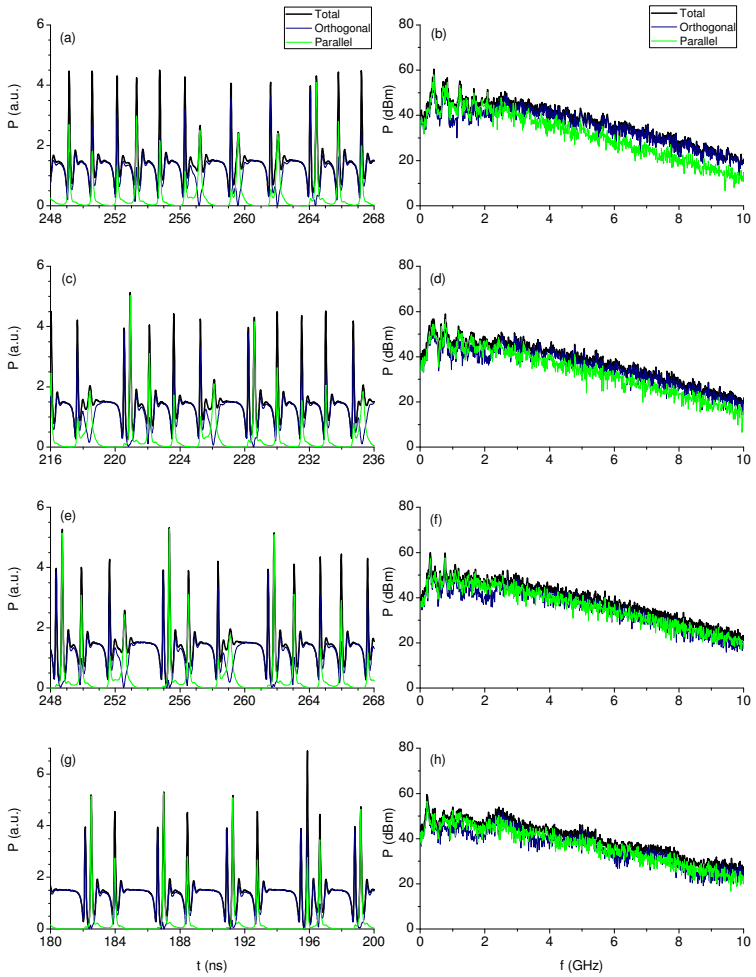

Figure 6: (left column): Temporal traces (right column): RF spectra. Total and both polarizations powers are shown. Values of E_{inj} are: (a,b) 0.0652, (c,d) 0.0655, (e,f) 0.066, (g,h) 0.067. Simulation with μ=2.44 and Δν=-2.7 GHz, with noise.

If the strength of injection is increased, an important effect of spontaneous emission noise can be seen in fig. 6(e)-(f). If these are compared to the corresponding case without noise (fig. 4(e)-(f)) is clear that the noise has totally broken the periodic dynamic and it has changed to an irregular regime, similar to the previous analyzed cases. The interpulse time deviation is now 840 ps. Finally, if the strength of injection is further increased, a very similar situation to fig. 4(g)-(h) is founded. Irregular and possibly chaotic dynamic is obtained. Temporal traces (fig. 6(g)) show irregular packets of pulses the RF spectra (fig. 6(h)) are very broad and have very weak peaks. Interpulse time deviation has a large value of 1033.6 ps.

As conclusion of this section, we can summarize some of our results. In the cases for -2 GHz frequency detuning, we have found a qualitative coincidence with the experimental results. The effect of spontaneous emission noise is, basically, to increase the interpulse time deviation. When the frequency detuning is -2.7 GHz and normalized bias current 2.44, behaviors are different to the previous ones. One of the most important results that we have found, without noise, is that the deterministic dynamics of the system shows complex nonlinear behaviors like period doubling, period three and also irregular and possibly chaotic regimes. It is interesting to note that although the system has not noise, standard deviation of interpulse time and the period is not a negligible value. On the other hand, the presence of noise can break the periodicity obtained without it.

IV. SUMMARY AND CONCLUSIONS

In this work we have presented a theoretical and experimental study of the polarization-resolved nonlinear dynamics of a 1550nm single-mode linearly polarized VCSEL when subject to orthogonal optical injection. Anticorrelated (correlated) dynamics between the two linear polarizations emitted by the VCSEL is found for negative (positive) frequency detuning. This behavior can be explained in terms of competence between polarizations [34]. The theoretical analysis has shown that irregular dynamics and appreciable values of interpulse time and period deviation can be found for negative frequency detuning in the deterministic system (i.e. without spontaneous emission noise). The effect of spontaneous emission noise on the dynamics, in general, is to increase the standard deviation of the interpulse time, and also in some cases it can change a periodic regime by an irregular one.

ACKNOWLEDGEMENTS

The authors acknowledge support from the Ministerio de Ciencia e Innovación under project TEC2009-14581-C02-02. Ana Quirce was supported in part by the Fondo Social Europeo (FSE) under the Junta de Ampliación de Estudios (JAE-Predoc) programme.

REFERENCES

[1] J. Ohtsubo, "Semiconductor lasers. Stability, instability and chaos". Springer series in optical sciences. Berlin 2007.
[2] F. Koyama, "Recent advances of VCSEL Photonics," *J. Lightwave Technol.* vol. 24, no. 12, pp. 4502-4513, Dec. 2006.
[3] C. J. Chang-Hasnain, J. P. Harbison, G. Hasnain, A. C. Von Lehmen, L. T. Florez, and N. G. Stoffel, "Dynamic, polarization and transverse mode characteristics of vertical-cavity surface-emitting lasers", *IEEE J. Quantum Electron*., vol. 27, no. 6, pp. 1402-1409, Jun. 1991.
[4] K. D. Choquette, R. P. Schneider, K. L. Lear, and R. E. Leibenguth, "Gain-dependent polarization properties of vertical-cavity lasers", *IEEE J. Select. Topics Quantum Electron*., vol. 1, no. 2, pp. 661-666, Mar./Apr 1995.
[5] R. Gordon, A. P. Heberle, J. R. A. Cleaver, "Transverse mode locking in microcavity lasers", *Appl. Phys. Lett*., vol. 81, no. 24, pp. 4523-4525, Dec. 2002.
[6] A. Valle, L. Pesquera, "Turn-off transients in current-modulated multitransverse-mode vertical-cavity surface-emitting lasers", *Appl. Phys. Lett*., vol. 79, no. 24, pp. 3914-3916, Dec. 2001.
[7] T. Kim, S. B. Kim, "Suppressing the turn-off induced pulsations in VCSELs using an elevated oxide-layer structure", *Opt. Exp.*, vol. 18, no.2, pp. 1271-1277, Jan. 2010.
[8] M. J. Adams, A. Hurtado, D. Labukhin, and I. D. Henning, "Nonlinear semiconductor lasers and amplifiers for all-optical information processing", *Chaos*, vol. 20, art. 037102, 2010.
[9] C. H. Chang, L. Chrostowski, C. J. Chang-Hasnain, "Injection locking of VCSELs," *IEEE J. Select. Topics Quantum Electron*., vol. 9, no. 5, pp.1386-1393, Sep./Oct 2003.
[10] D. Parekh, X. Zhao, W. Hofmann, M. C. Amann, L. A. Zenteno and C. J. Chang-Hasnain, "Greatly enhanced modulation response of injection-locked multimode VCSELs," *Opt. Exp.,* vol. 16, no. 26, pp. 21582-21586, Dec. 2008.
[11] D. Parekh, B. Zhang, X. Zhao, Y. Yue, W. Hofmann, M.C. Amann, A. Willner, and C. J. Chang-Hasnain, "Long distance single-mode fiber transmission of multimode VCSELs by injection locking", *Opt. Exp.*, vol. 18, no.20, pp. 20552-20557, 2010.
[12] H. Li, T. Lucas, J. G. McInerney, M. Wright, and R. A. Morgan, "Injection locking dynamics of vertical cavity semiconductor lasers under conventional and phase conjugate injection. "*IEEE J. Quantum Electronics*, vol. 32, no. 3, pp. 227-235, Feb. 1996.
[13] Y. Hong, P. S. Spencer, S. Bandyopadhyay, P. Rees, and K. A. Shore, "Polarization resolved chaos and instabilities in a VCSEL subject to optical injection", *Opt. Comm.*, vol. 216, pp. 185-187, 2003.
[14] Z. G. Pan, S. Jiang, M. Dagenais, R. A. Morgan, K. Kojima, M. T. Asom, and R. E. Leibenguth, "Optical injection induced polarization bistability in vertical-cavity surface-emitting lasers," *Appl. Phys. Lett*., vol. 63, no. 22, pp. 2999-3001, Nov.1993.

[15] D. L. Boiko, G. M. Stéphan, and P. Besnard, "Fast polarization switching with memory effect in a vertical cavity surface emitting laser subject to modulated optical injection," *J. Appl. Phys*. 86, pp. 4096–4099, Oct. 1999.
[16] Y. Hong, K.A. Shore, A. Larsson, M. Ghisoni, and J. Halonen, "Pure frequency-polarisation bistability in vertical-cavity surface-emitting lasers subject to optical injection", *Electron. Lett.* 36, no. 24, pp. 2019-2020, 2000.
[17] Y. Hong, P.S. Spencer, P. Rees and K.A. Shore, "Optical injection dynamics of two-mode vertical cavity surface-emitting semiconductor lasers", *IEEE J. Quantum Electronics*, vol. 38, no. 3, pp. 274-278, Mar. 2002.
[18] J. Buesa, I. Gatare, K. Panajotov, H. Thienpont, and M. Sciamanna, "Mapping of the dynamics induced by orthogonal optical injection in vertical-cavity surface-emitting lasers", *IEEE J. Quantum Electron*., vol. 42, no. 2, pp. 198-207, Feb. 2006.
[19] I. Gatare, J. Buesa, H. Thienpont, K. Panajotov, M. Sciamanna, "Polarization switching bistability and dynamics in vertical-cavity surface-emitting lasers under orthogonal optical injection", *Optical and Quantum Electronics*. 38, pp. 429-443, 2006.
[20] I. Gatare, K. Panajotov, M. Sciamanna, "Frequency-induced polarization bistability in vertical-cavity surface-emitting lasers with orthogonal optical injection", *Phys Rev. A*. 75, 023804, 2007.
[21] M. Sciamanna and K. Panajotov, "Route to polarization switching induced by optical-injection in vertical-cavity surface-emitting lasers", *Phys. Rev. A*, vol. 73, no. 2, 023811, Feb. 2006.
[22] I. Gatare, M. Sciamanna, M. Nizette, and K. Panajotov, "Bifurcation to polarization switching and locking in vertical-cavity surface-emitting lasers with optical injection", *Phys. Rev. A*, vol. 76, no. 031803(R), 2007.
[23] K. Panajotov, I. Gatare, A. Valle, H. Thienpont and M. Sciamanna, "Polarization- and Transverse-Mode Dynamics in Optically Injected and Gain-Switched Vertical-Cavity Surface-Emitting Lasers", *IEEE J. Quantum Electron.* vol.45, no.11, pp.1473-1481, Nov. 2009.
[24] I. Gatare, M. Sciamanna, M. Nizette, H. Thienpont and K. Panajotov, "Mapping of two-polarization-mode dynamics in vertical-cavity surface-emitting lasers with optical injection," *Phys. Rev. E*., vol. 80, no. 026218, Aug. 2009.
[25] M. Nizette, M. Sciamanna, I. Gatare, H. Thienpont, and K. Panajotov, "Dynamics of vertical-cavity surface-emitting lasers with optical injection: a two-mode model approach", *J. Opt. Soc. Am. B*, vol. 26, no. 8, pp. 1603-1613, Aug. 2009.
[26] A. Valle, M. Gomez-Molina, and L. Pesquera, "Polarization bistability in 1550 nm wavelength single-mode vertical-cavity surface-emitting lasers subject to orthogonal optical injection," *IEEE J. Sel. Top in Quantum Electron.*, vol. 14, no. 3, pp. 895-902, May/Jun.2008.
[27] A. Hurtado, I. D. Henning, and M. J. Adams, "Two-wavelength switching with a 1550 nm VCSEL under single orthogonal optical injection," *IEEE J. Sel. Top. in Quantum Electron*, vol. 14, no. 3, pp. 911-917, May/Jun.2008.
[28] K. H. Jeong, K. H. Kim, S. H. Lee, M. H. Lee, B. S. Yoo and K. A. Shore, "Optical injection-induced polarization switching dynamics in 1.5 μm wavelength single-mode vertical-cavity surface-emitting lasers," *IEEE Photon. Technol. Lett.,* vol. 20, no. 9-12, pp. 779-781, May. 2008.
[29] A. Quirce, A. Valle, and L. Pesquera, "Very wide hysteresis cycles in 1550 nm-VCSELs subject to orthogonal optical injection", *IEEE Phot. Tech. Lett*. 21, no. 17, pp. 1193-1195, 2009.
[30] A. Hurtado, A. Quirce, A. Valle, L. Pesquera, and M. J. Adams, "Power and wavelength polarization bistability with very wide hysteresis cycles in a 1550nm-VCSEL subject to orthogonal optical injection", *Opt. Exp*. 17, no. 26, pp. 23637-23642, 2009.
[31] A. Hurtado, A. Quirce, A. Valle, L. Pesquera, and M. J. Adams, "Nonlinear dynamics induced by parallel and orthogonal optical injection in 1550 nm vertical-cavity surface-emitting lasers (VCSELs)", *Opt. Exp*., vol. 18, no. 9, pp. 9423-9428, 2010.
[32] P. Perez, A. Quirce, L. Pesquera, and A. Valle, "Polarization resolved nonlinear dynamics induced by orthogonal optical injection in long-wavelength VCSELs", *IEEE J. Sel. Top. Quantum Electron.* vol. 17, pp.1228-1235, Nov. 2011
[33] R. Al-Seyab, K. Schires, N. A. Khan, A. Hurtado, I. D. Henning, and M. J. Adams, "Dynamics of polarized optical injection in 1550 nm VCSELs: theory and experiments", *IEEE J. Sel. Top. Quantum Electron.* vol. 17, pp.1242-1249, Nov. 2011
[34] A. Quirce, P. Perez, A. Valle, and L. Pesquera, "Correlation properties and time-resolved dynamics of linear polarizations emitted by single-mode vertical-cavity surface-emitting lasers subject to orthogonal optical injection", *J. Opt. Soc. Am. B*, vol. 28, no. 11, pp. 2765-2776, Nov. 2011.
[35] A. Quirce, P. Perez, A. Valle, and L. Pesquera, "Optical spectral analysis of the nonlinear dynamics in long-wavelength single-mode VCSELs subject to orthogonal optical injection", *SPIE Photonics West*, Conference on Physics and Simulation of Optoelectronics Devices XIX, San Francisco, USA, 21-26 January 2012.

[36] J. M. Martín-Regalado, F. Prati, M. San Miguel, N. B. Abraham, “Polarization properties of vertical-cavity surface-emitting lasers”, *IEEE J. Quantum Electron*, vol. 33, pp. 765-783, May 1997.